# STM and Raman spectroscopic study of graphite irradiated by heavy ions

J. Liu [a,*], M.D. Hou [a], C. Trautmann [b], R. Neumann [b], C. Müller [b],
Z.G. Wang [a], Q.X. Zhang [a], Y.M. Sun [a], Y.F. Jin [a], H.W. Liu [c], H.J. Gao [c]

[a] *Institute of Modern Physics, Chinese Academy of Sciences (CAS), Lanzhou 730000, China*
[b] *Gesellschaft für Schwerionenforschung (GSI), Planckstr. 1, 64291 Darmstadt, Germany*
[c] *Institute of Physics, Chinese Academy of Sciences (CAS), Beijing 100080, China*

## Abstract

Highly oriented pyrolytic graphite was irradiated with swift heavy ions (Ne, Cr, Fe, Ni, Zn, Xe and U) of fluences between $10^{11}$ and $10^{14}$ ions/cm$^2$ in energy range MeV–GeV. The combination of scanning tunneling microscopy (STM) and Raman spectroscopy studies shows that large numbers of tracks protrude from the surface. The disordered crystal lattice is leading to a Raman-active D mode. Quantitative analysis of the peak intensity indicates that the size of the crystallite domain is larger than the mean distance between in-plane tracks observed by STM.
© 2003 Elsevier B.V. All rights reserved.

*PACS:* 61.80.Jh; 68.37.Ef; 87.64.Je
*Keywords:* Graphite; Heavy ions; Scanning tunnel microscopy; Raman spectroscopy

## 1. Introduction

When a swift heavy ion penetrates into a solid, it induces along its trajectory a cylindrical zone of ionizations and electronic excitations. In many insulating crystals as well as in non-metallic electronically conductive solids with a layered structure such as germanium sulfide [1] and graphite, electron–phonon coupling causes the displacement of atoms leading to lattice disorder in many cases up to amorphisation [2–7] and structural rearrangement.

As we recently showed [8] ion tracks created on the surfaces of highly oriented pyrolytic graphite (HOPG) by different ions in the energy range MeV–GeV exhibit rather small diameters between 2.0 and 3.5 nm compared to other materials. In addition, it was interesting to see that the probability for track formation is a function of the electronic energy loss $(dE/dx)_e$. A situation where each projectile creates a surface track requires a critical energy loss of 18 keV/nm. Below this threshold, the creation yield strongly declines with decreasing $(dE/dx)_e$ (Fig. 7 in [8]). We concluded that ion tracks in HOPG are not homogeneous cylindrical damage trails but rather consist of a discontinuous sequence of defect zones.

Since studies of the surface development after high fluence ion irradiation can be useful for better

---

* Corresponding author. Tel.: +86-931-4969331; fax: +86-931-4969201.
*E-mail address:* j.liu@impcas.ac.cn (J. Liu).

understanding of surface sputtering, diffusion and modification. In this work, we are interested in effects and defects induced by various energetic heavy ions of fluence $10^{11}$ to $10^{14}$ ions/cm$^2$ in HOPG. In addition to scanning tunneling microscopy (STM) studies of the HOPG surface damage, this paper focuses on the presentation of new Raman scattering results on ion irradiation because it is sensitive to structural disorder occurred within optical skin depth of a laser beam [9–11]. The crystallite domain size can be estimated quantitatively in terms of D-peak intensity in Raman spectrum.

## 2. Experimental

Freshly cleaved HOPG crystals (provided by Advanced Ceramics Co.) were irradiated with Ni, Zn, Xe and U ions of specific energy 11.4 MeV/u at the linear accelerator UNILAC and with Ne, Cr, Zn, Xe ions (1.4 MeV/u) at the high-charge injector HLI, both facilities being operated at GSI, Darmstadt. The irradiation with Fe ions was performed at the cyclotron HIRFL (22 MeV/u) of IMP, Lanzhou. In some cases, aluminum degrader foils of different thicknesses were placed in front of the samples. This allowed us to vary the energy of a given ion beam between GeV and several MeV, corresponding to electronic energy loss values between 2 and 30 keV/nm. The ion flux was in the range of $8 \times 10^7 – 4 \times 10^8$ ions/cm$^2$ s. Depending on the ion species, fluences between $4 \times 10^{11}$ and $2.2 \times 10^{14}$ ions/cm$^2$ were applied. All irradiations were performed at room temperature and under beam incidence normal to the $c$-plane of the samples.

After irradiation, the surface of the crystals was imaged using both a home-built STM and a commercial Solver P47 SPM from NT-MDT Company. The microscopes were operated in a constant-current mode in air. As sensors, we used mechanically sharpened Pt/Ir tips and chemically etched tungsten tips, respectively.

A Microscopic Confocal Raman Spectrometer Renishaw RM2000 was used to characterize the pristine and ion-irradiated graphite. The excitation source was a 514.5 nm Ar-ion laser with power 20

mW. For such a wavelength, the optical skin depth in graphite is approximately 50 nm. The back-scattered radiation was collected normal to the sample surface. Microscope with 50× objective lens was used which allows a spatial resolution of 2 μm. The resolution of a spectrum is 1 cm$^{-1}$. The full width at half maximum (FWHM) and the integrated intensity of the peaks were determined using Lorentzian fitting.

## 3. Results and discussion

STM images of different samples irradiated with only high fluence U, Xe, Cr and Ne ions are shown in Fig. 1. The dense ion tracks appear as circular objects of increased contrast. Based on earlier results by several other groups [12–18], it is predominantly ascribed to an increased topographical signal, i.e. the impinging ions create hillock-like features. The surface crystalline structure was partially disordered, whereas the original basal-plane orientation is still maintained. The different contrast in image Fig. 1(d) is due to the higher fluence incidence of ions. In the center of the impact zone, the lattice structure cannot be resolved due to severe damage. Taking into account a track diameter of 2 nm and a covalent radius of carbon atoms of 0.08 nm, the number of carbon atoms involved in a damage cross-section is about one hundred.

As mentioned, the yield $\xi$ for track creation (i.e. number of observed tracks compared to ion fluence applied) is a function of $(dE/dx)_e$. For a given fluence, the observable track density is therefore rather small for light ions with low energy losses. This is obvious if we compare the four images in Fig. 1, where the track densities are approximately the same although the irradiation fluence of Ne ions with $(dE/dx)_e = 2.5$ keV/nm was almost 3 orders of magnitude larger than that of U ions with $(dE/dx)_e = 29.7$ keV/nm. The track creation yields are 1.1, 1.0, $1.2 \times 10^{-1}$ and $1.8 \times 10^{-3}$, respectively.

The Raman spectra of HOPG before and after the irradiation with respect to Cr and Ne, Xe, U ions are presented in Figs. 2 and 3. The observed Raman spectrum is made up of the superposition
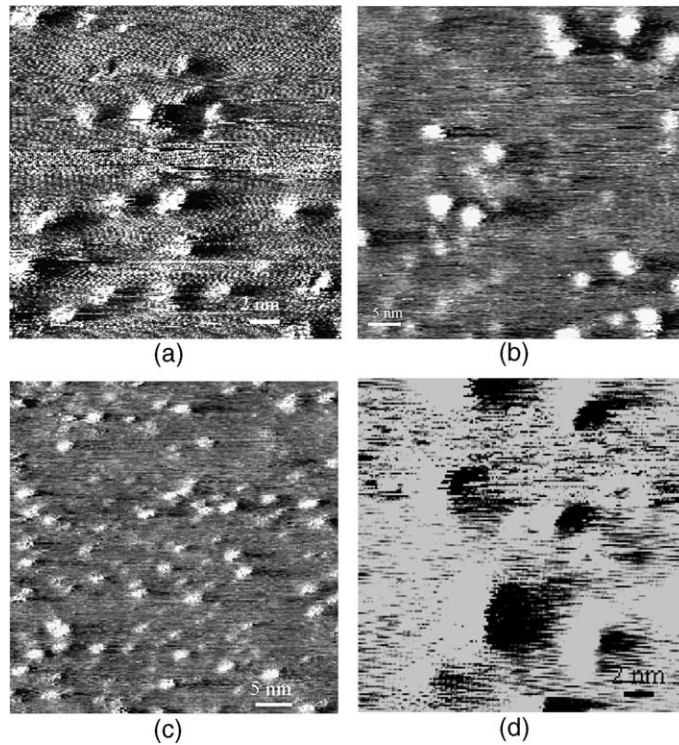
Fig. 1. STM micrographs recorded on graphite surfaces irradiated with (a) 1160 MeV U ions of fluence $\phi = 8 \times 10^{11}$ ions/cm$^2$; (b) 802 MeV Xe ions, $\phi = 1.5 \times 10^{12}$ ions/cm$^2$; (c) 37 MeV Cr ions, $\phi = 3 \times 10^{13}$ ions/cm$^2$ and (d) 31 MeV Ne ions, $\phi = 2.2 \times 10^{14}$ ions/cm$^2$.

of scattering from both damaged and undamaged area. The virgin spectrum is dominated by a sharp band at 1580 cm$^{-1}$ (G mode) assigned to the Raman-active $E_{2g}$ mode [9–11]. After ion irradiation the extra first-order lines, corresponding to high-density phonon states, are usually designated as D modes. New peaks at 1346 (shoulder, D$_1$), 1367 (D$_2$) and 1622 (shoulder, D$'$) cm$^{-1}$ are originated from the onset of disorder [19]. Note that the D mode comes only when the irradiation fluence $\phi$ surpasses a critical value $\phi_c$, which is smaller for heavier projectiles with higher energy loss.

Ion irradiation is expected to cause a decrease in G mode intensity and increase D mode intensities. The radiation-induced D$_2$ line is wider compare to G line as shown in Fig. 4(a). FWHM of D$_2$ increases from a value of 19–22 cm$^{-1}$ while the fluences of Cr ions varying from $1 \times 10^{13}$ to $3 \times 10^{13}$ ions/cm$^2$. In Fig. 4(b), the ratio of integrated area of all D lines to G is increasing, indicating an increase of damage in the samples. From
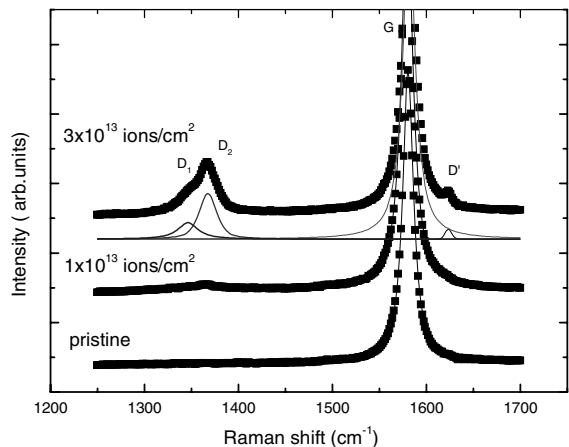


Fig. 2. Raman spectra of pristine HOPG and samples irradiated with 73 MeV Cr ions of two fluences.

the magnitude of the relative intensities $R$ of D line with respect to G line, the size of the ordered crystallite domains $L_a$ can be determined. For laser
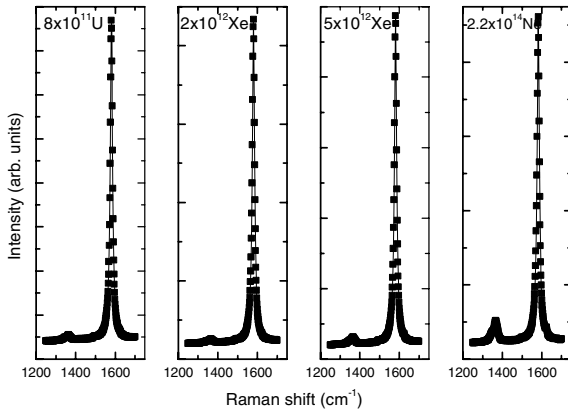
Fig. 3. Raman spectra of HOPG irradiated with 1160 MeV U ions to a fluence of $\phi = 8 \times 10^{11}$ ions/cm$^2$, 190 MeV Xe ions $\phi = 2 \times 10^{12}$ and $5 \times 10^{12}$ ions/cm$^2$ and 31 MeV Ne ions $\phi = 2.2 \times 10^{14}$ ions/cm$^2$.
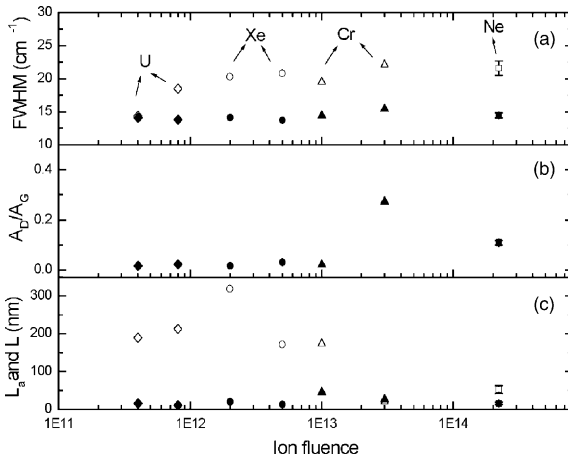


Fig. 4. Analysis of the Raman spectra of samples irradiated by U, Xe, Cr and Ne ion irradiation: (a) FWHM of $D_2$ peak (open symbol) and G peak (solid symbol); (b) ratio of integrated area of D–G; (c) the lattice domain size $L_a$ (open symbol) and the mean distance between in-plane tracks $L$ (solid symbol) as function of ion fluences. The errors from data fitting are 5% and 3% for FWHM of D and G peaks, 10% for $A_D/A_G$ and 20% for $L_a$ and $L$, respectively.

light of 514.5 nm, $R = 4.4/L_a$ (nm) [20]. In our case, $L_a$ rapidly decreases from $L_a \sim 1$ μm for virgin HOPG to about 20 nm for sample irradiated with 73 MeV Cr ions to a fluence of $3 \times 10^{13}$ ions/cm$^2$ (Fig. 4(c)). The other's results have shown that the in-plane phonon correlation length is equal to

the mean distance between defects [21]. Here ion tracks terminate the spatial extension optical phonon in graphite plane. The mean distance between in-plane tracks is given by $L = 1/(\xi \times \phi)^{1/2}$, where $\xi$ is the track yield from STM measurement and $\phi$ is the ion fluence. It is obvious that the domain size $L_a$ in the range of 20–300 nm is larger than $L$ of 10–50 nm in our experiment except the very high-fluence ion irradiation conditions. Since $L_a$ is an average value in near-surface region from Raman measurement, it can be concluded that the damage on the surface is more severe compared with in the near-surface region. It confirms our previous results, i.e. the track formation is significantly reduced inside the material compared to the original surface. A more refined analysis needs to be performed for better understanding Raman spectra in combination with the size and morphology of the tracks of different ion species.

## 4. Conclusions

When swift heavy ions penetrate the surface of HOPG crystals, they create small hillocks of diameter 2–3.5 nm. STM images clearly show that in the central part of the impact zone, the ordered structure of the graphite lattice is destroyed. Additional evidence for lattice disorder is found in the Raman spectra of high-fluence samples. When accumulated disorder reaches a level, the disorder-induced D mode appears in Raman spectra. Quantitative analysis of the D-peak intensity indicates a decrease of the crystal domain size at higher ion fluence. Comparing it with the mean distance between in-plane tracks, we can conclude that the track formation is significantly reduced in the near surface region.

## Acknowledgements

# References

[1] J. Vetter, R. Scholz, D. Dobrev, L. Nistor, Nucl. Instr. and Meth. B 141 (1998) 747.

[2] V. Chailley, E. Dooryhee, M. Levalois, Nucl. Instr. and Meth. B 107 (1996) 199.

[3] L. Douillard, J.P. Duraud, Nucl. Instr. and Meth. B 107 (1996) 212.

[4] B. Canut, S.M.M. Ramos, R. Brenier, P. Thévenard, J.L. Loubet, M. Toulemonde, Nucl. Instr. and Meth. B 107 (1996) 194.

[5] Y.F. Jin, R.H. Xu, J.M. Quan, Z.G. Wang, Q.H. Meng, Y.M. Sun, F. Ma, J. Han, G. Liu, J. Liu, C.L. Li, Nucl. Instr. and Meth. B 107 (1996) 227.

[6] M. Toulemonde, Ch. Dufour, A. Meftah, E. Paumier, Nucl. Instr. and Meth. B 166–167 (2000) 903.

[7] G. Schiwietz, E. Luderer, G. Xiao, P.L. Grande, Nucl. Instr. and Meth. B 175–177 (2001) 1.

[8] J. Liu, R. Neumann, C. Trautmann, C. Müller, Phys. Rev. B 64 (2001) 184115.

[9] K. Nakamura, M. Kitajima, Phys. Rev. B 45 (1992) 5672.

[10] B.S. Elman, G. Braunstein, M.S. Dresselhaus, G. Dresselhaus, T. Venkatesan, J.M. Gibson, Phys. Rev. B 29 (1984) 4703.

[11] B.S. Elman, M. Shayegan, M.S. Dresselhaus, H. Mazurek, G. Dresselhaus, Phys. Rev. B 25 (1982) 4142.

[12] L. Porte, M. Phaner, C.H. de Villeneuve, N. Moncoffre, J. Tousset, Nucl. Instr. and Meth. B 44 (1989) 116.

[13] R. Coratger, A. Claverie, F. Ajustron, J. Beauvillain, Surf. Sci. 227 (1990) 7.

[14] J. Yan, Z. Li, C. Bai, W.S. Yang, Y. Wang, W. Zhao, Y. Kang, F.C. Yu, P. Zhai, X. Tang, J. Appl. Phys. 75 (1994) 1390.

[15] J.R. Hahn, H. Kang, Phys. Rev. B 60 (1999) 6007.

[16] H. Kemmer, S. Grafström, M. Neitzert, M. Wörtge, R. Neumann, C. Trautmann, J. Vetter, N. Angert, Ultramicroscopy 42–44 (1992) 1345.

[17] S. Bouffard, J. Cousty, Y. Pennec, F. Thibaudau, Radiat. Eff. Def. Sol. 126 (1993) 225.

[18] L.P. Biró, J. Gyulai, K. Havancsák, Phys. Rev. B 52 (1995) 2047.

[19] P. Tan, Y. Deng, Q. Zhao, W. Cheng, Appl. Phys. Lett. 74 (1999) 1818.

[20] D.S. Knight, W.B. White, J. Mater. Res. 4 (1989) 385.

[21] E. Asari, I. Kamioka, K.G. Nakamura, T. Kawabe, W.A. Lewis, M. Kitajima, Phys. Rev. B 49 (1994) 1011.